Radiotracers Available for Cancer and Disease

Subjects: Cell Biology

Contributor: Yi-Fang Yang , Chien-Hsiu Li , Huei-Yu Cai , Bo-Syuan Lin , Cheorl-Ho Kim , Yu-Chan Chang

Various factors have been linked to abnormal metabolic reprogramming, including gene mutations, epigenetic modifications, altered protein epitopes, and their involvement in the development of disease, including cancer. The presence of multiple distinct hallmarks and the resulting cellular reprogramming process have gradually revealed that these metabolism-related molecules may be able to be used to track or prevent the progression of cancer. Consequently, translational medicines have been developed using metabolic substrates, precursors, and other products depending on their biochemical mechanism of action. It is important to note that these metabolic analogs can also be used for imaging and therapeutic purposes in addition to competing for metabolic functions. In particular, due to their isotopic labeling, these compounds may also be used to localize and visualize tumor cells after uptake.

cancer metabolism metabolic reprogramming molecular imaging cellular uptake

1. Introduction

The microenvironment, immune system, and signaling pathways are abnormal in cancer and other diseases and have been shown to be closely related to metabolic events [1]. In particular, subpopulations of lesions themselves are particularly dependent on specific nutrients and increase the rate of absorption and generation. Because of this property, many radiotracers that have been developed based on metabolites can be used for visualization, localization, and quantification (**Figure 1** and **Figure 2**).

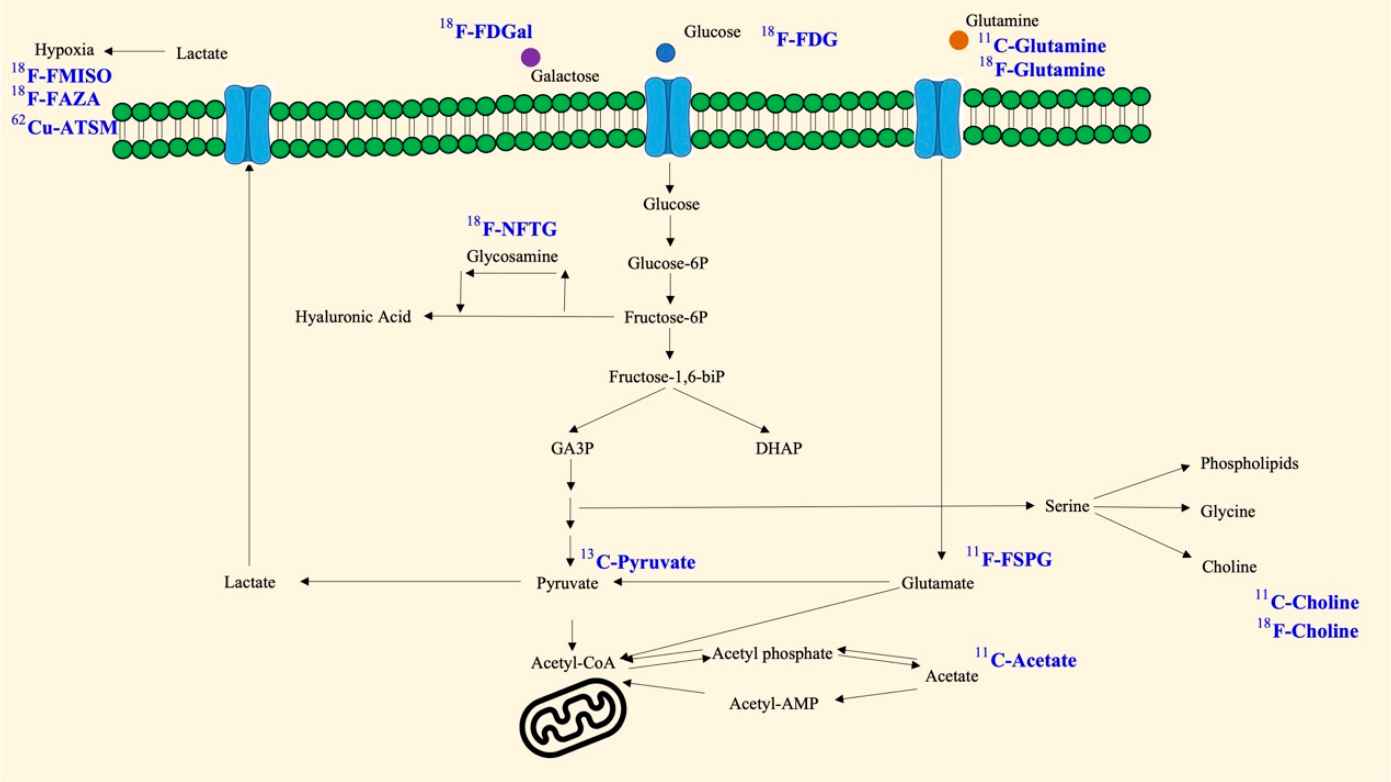

Figure 1. Available metabolism-based radiotracers and their background. The schematic model shows that monosaccharides (glucose and galactose) and glutamine can be taken up by cells, followed by cascade catalysis and synthesis. Glucosamine, pyruvate, glutamate, acetate, and choline may be intermediates or have further consequences. Furthermore, hypoxia is a metabolic reprogramming event with corresponding detectable targets. The blue color represents the derived radiotracer products.

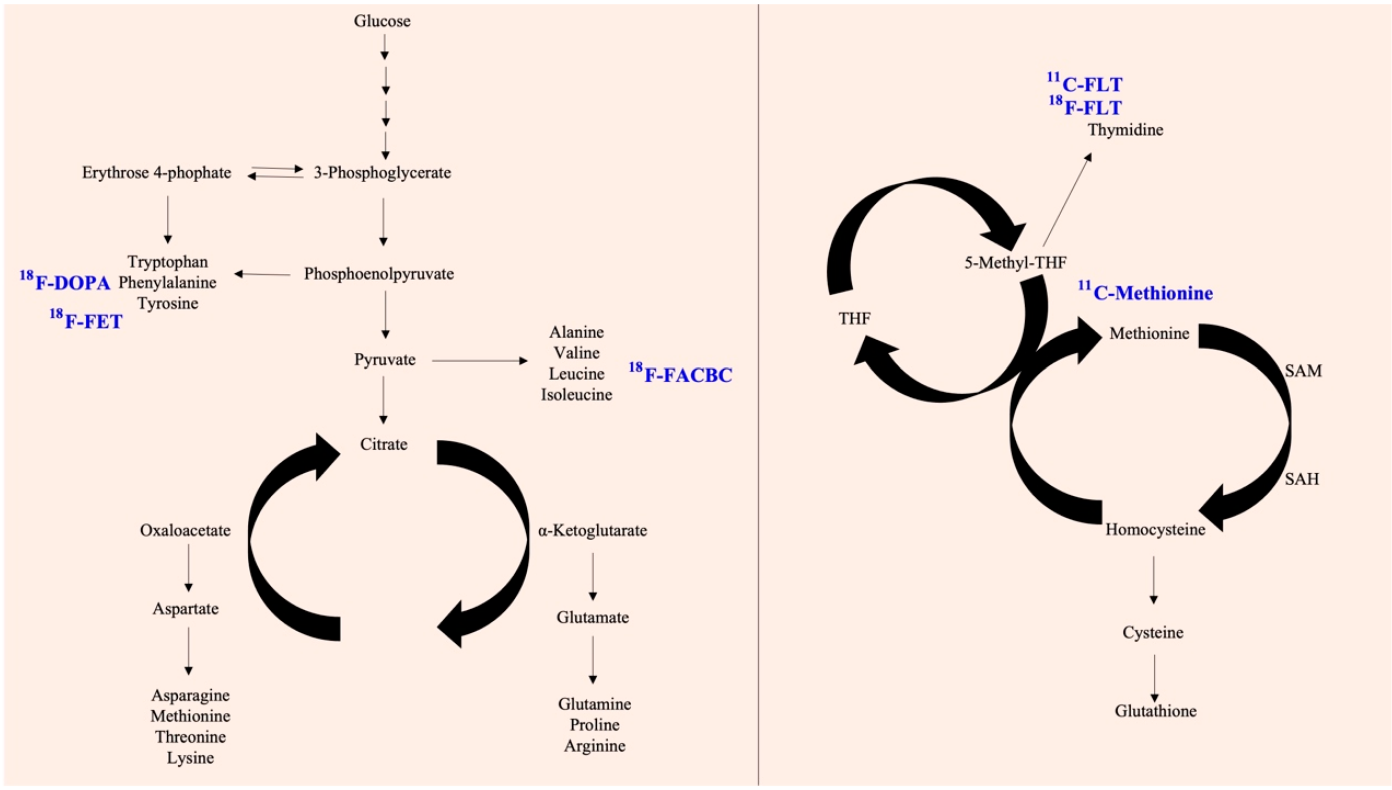

Figure 2. Available metabolism-based radiotracers and their background. The schematic model shows glycolysis and the further TCA cycle, amino acid biosynthesis. In the path, there are some potential targets with radiotracers (**left panel**). In addition, the coupling of the folate cycle to the methionine cycle is shown (**right panel**). The blue color represents the derived radiotracer products.

2. Glucose

Glycolysis is a pathway that uses glucose for metabolism and catalysis, and there are many related studies and evidence. Scientists have found that there are many diseases and cancers associated with abnormal glycolysis. The unbalanced proliferation activity of tumor cells results in increased glucose uptake by tumor cells. This includes not only an increase in the glucose uptake rate, but also an increase in the efficiency of the transporter responsible for the membrane [2].

Several clinical studies, such as The Cancer Genome Atlas (TCGA) and Gene Expression Omnibus, have demonstrated that certain cancer types exhibit selective overexpression of glucose transporters (GLUTs). It was found in Kim's research that the expression of GLUT2 was significantly higher in hepatocellular carcinomas than in normal tissues when compared with other submembers of the GLUT family. Accordingly, this difference is positively correlated with poor prognosis or clinical stage of patients, thus it may serve as a prognosis factor [3]. It has been found that GLUT3 is overexpressed in several carcinomas, including adenocarcinoma and glioblastoma [4][5][6].

The downstream genes responsible for the 10 steps of the glycolysis response will also follow this pattern by increasing their enzyme activity and expression levels [7], consequently activating several signaling transduction pathways and transcription factors. This process is encapsulated in the Warburg effect theory to accelerate glucose/lactate conversion to respond to oxygen concentrations in tumor cells [8].

In highly proliferating specific cells, there is a specific difference between glucose uptake and glycolysis rates. This has led to the development of molecules that target glucose for use as markers. Fluorodeoxyglucose (FDG) is an analog of a glucose molecule, similar in structure to glucose. FDG is taken up via the GLUT-1 transporter and phosphorylated to FDG-6-phosphate by hexokinase [9]. Because of the lack of C-2 hydroxyl groups, further metabolism is impeded, and the FDG-6-phosphate is trapped within cells, accumulates at high absorption, and is eventually metabolized. Many basic and clinical studies have used FDG as an inhibitor to interfere with the normal glycolysis reaction by selecting specific cells with high sugar uptake. Radiation scientists also use the abovementioned imaging equipment. Radiolabeling technology has been used to design products such as ^{18}F-FDG, which is derived from PET and can track the FDG signal to locate the tumor location. The advantage of FDG-PET is that it can be used as an early assessment of whether the tumor metabolism has changed and to evaluate whether a change in treatment strategy is necessary [10]. As a matter of fact, this depends on the high glycolytic rate of the tumor or disease model, if the glycolytic rate is insufficient, there will be no significant difference in the degree of contrast in imaging [10][11].

There are many other modifications and improvements of FDG, including radioisotopes, peptides (linear and cyclic), and some conjugations [12]. Namavari et al. used ^{18}F-FDG as a prosthetic set to design ^{18}F-FDG-RGD and ^{18}F-FDG-cyclo (RGDDYK) by one-step radiosynthesis. This design can increase the binding affinity to the integrin $\alpha_v\beta_3$. The imaging of integrin αvβ3 expression in vivo is a potentially useful method for diagnosing tumors and their metastases to provide a better understanding of tumor angiogenesis and monitor the effects of target-specific antiangiogenic therapy. Senisik et al. also describe a single-step, high-efficiency conjugation of glycylglycine (GlyGly), which is a small peptide, with [^{18}F] FDG, without the need for purification. Researchers without cyclotron facilities can easily perform efficient radiolabeling and use [^{18}F] FDG-GlyGly to improve biodistribution studies [13].

Whole body scans are mainly used for tumor examination. It is recommended that the patient fast for a minimum of six hours before the test and maintain a blood sugar level less than 120 mg/dL. After intravenous injection of about 5 to 10 millicuries (mCi) of FDG, the subject must lie down and rest for 45 min, so that the FDG can accumulate in the tumor, be adequately eliminated from normal tissues, and pass through the kidneys and bladder [14]. After 45 min of excretion, after removal of urine, the patient lies down on the scanning table for examination. Generally, it takes about an hour to scan from the head to the upper third of the thigh [15]. To reduce the influence of body tissue on the attenuation effect of gamma rays, a ^{68}Ge radiation source is generally used for another transmission scan to correct the tissue attenuation effect, and an additional 15 to 30 min of examination time is required. After scanning, tomographic image reconstruction and analysis can be performed [16]. If necessary, the absorption rate of FDG by the lesion, such as the standard uptake value (SUV), can be measured. There is the option for a local scan to be added, and the examination time for this is approximately 20 min, to allow for the differential diagnosis of benign and malignant lesions in specific organs (such as lung masses).

3. Pyruvate

In the glycolytic pathway, lactate and pyruvate act as two branches, leading to glycolysis and anaerobic lactic fermentation or aerobic oxidative phosphorylations (OXPHOs) [17]. The conversion of glucose to pyruvate occurs through glycolysis in cancer, whereas lactate is produced by lactate dehydrogenase (LDH) [18]. In this manner, cancer cells are exploited for their unique properties. It has been reported that some studies have attempted to increase detection sensitivity in solution-state nuclear magnetic resonance experiments by using dynamic nuclear polarization of ^{13}C-labeled pyruvate [19]. In vivo imaging of the spatial distribution and metabolism of a labeled molecule following intravenous injection in mouse models is possible by using ^{13}C magnetic resonance spectroscopic imaging (MRSI). In a reaction catalyzed by LDH, the decrease in label flux between hyperpolarized [1-^{13}C]pyruvate and lactate can be measured to determine whether mouse lymphomas are responding to drug treatment. There may be several reasons for the reduction in flux, such as loss of cell enzymes, reduced tumor cellularity, or reduced concentrations of lactate and NAD(H) in the tumor. Therefore, it is important to compare these results with FDG-PET to improve the value of FDG-PET in its current board-certified clinical application [20].

4. Galactose

A variety of cancers have been successfully treated using the combination of ^{11}C-acetate and FDG PET/CT. However, the detection sensitivity of HCC types for the small primary subtype is low [21]. Several studies have demonstrated that HCC has a greater effect on food intake and galactose production within the body. The expression of galactose metabolism related enzymes such as galactokinase (GALK1) and galactose-1 phosphate uridylyltransferase (GALT) in HCC is higher than that of normal liver tissues and is critical for HCC proliferation [22]. It has been demonstrated that galactose is metabolized specifically in hepatocytes, and thus a proof-of-concept imaging test has been developed for the diagnosis of liver cancer [23]. Compared with other tracers, 2-deoxy-2-[^{18}F]fluoro-D-galactose ([^{18}F]FDGal) was found to accumulate in the liver more frequently [24][25]. FDGal can be synthesized using commercially available FDG production kits with only minor modifications, enabling this process to be implemented at most clinical PET facilities [26]. ^{18}F-FDGal PET/CT was able to detect previously unknown extrahepatic diseases and regions when used in conjunction with contrast enhancement CT (ce-CT) for liver lesions. [23]. Despite this, the ^{18}F-FDGal PET/CT images are still limited by the extremely high uptake of ^{18}F-FDGal in normal liver tissue as well as by the heterogeneity of uptake in cirrhosis patients. A comparison and discussion of three ^{18}F-FDGal PET protocols was conducted by Horsager et al., in order to achieve the highest tumor/background ratio and optimal observations [27]. Furthermore, some studies have noted that coadministration does not improve the interpretation, detection, or statistical values of ^{18}F-FDGal PET/CT images [28].

5. Choline

A nutrient that builds cell membranes and phospholipids, choline, is necessary for brain development and memory, and is a precursor to acetyl-CoA, which is involved in muscle control and neuronal transmission. The activity of choline metabolism-related metabolic enzymes is abnormally increased in cancer and is related to malignancy. Activated phosphatidylcholine-specific phospholipase D (PC-PLD) and phospholipase C (PC-PLC) are associated with abnormal tumor proliferation in ovarian cancer [29]. Increased levels of glycerophosphorylcholine (GPC) and phosphorylcholine (PC) promote epithelial-to-mesenchymal transition (EMT) in ovarian cancer [30]. In some studies, highly saturated phosphatidylcholine species, CDP-choline species, and phosphocholine species are significantly higher in HCC tumors than in adjacent liver and intrahepatic cholangiocarcinoma (ICC) tumors [31].

Fluorine (18F) has been labeled for PET and CT to detect chronic liver diseases and liver cancers [32]. Despite having a similar function to ^{18}F-FDGal, ^{18}F-fluorocholine uptake shows significant associations with liver uptake and neuroinflammatory and fibrotic changes found in chronic liver disease patients' histology [32].

Choline can also be labeled with carbon-11 (^{11}C) as a positron emitter for molecular imaging [33]. Among several short-lived positron-emitting radionuclides used in PET imaging, ^{11}C has a unique probability (t1/20.4 min, $E_{\beta+}$ = 1.98 MeV) that is easily distinguished from the nonradioactive ^{12}C molecule. In addition, ^{11}C has a short half-life (20.33 min) and most ^{11}C will decay into ^{11}B through β decay, which is less harmful to the human body and has increased applicability [34]. Evaluation of *N*-methyl-[^{11}C]choline in PET in patients with recurrent prostate cancer and localized parathyroid adenomas that exhibit biochemical recurrence has been performed. It has been evidenced that the choline kinase alpha (XKα) overexpression can be found in primary hyperparathyroidism, parathyroid hyperplasia, and neoplastic lesions [35]. Liu et al. evaluated the value of ^{11}C-choline PET in patients

with primary hyperparathyroidism and indicated that this tool had potential for the location of parathyroid adenomas when ultrasound and ^{99m}Tc-sestamibi imaging yielded negative or discordant results [36]. Although the study by Noltes et al. was a retrospective analysis, the results were still promising, showing high accuracy and sensitivity [37]. Furthermore, ^{11}C-choline PET can also be applied to prostate cancer. Although serum prostate specific antigen (PSA) testing is often used to monitor disease recurrence after definitive therapy for prostate cancer [38], Krause et al. identified a positive correlation between ^{11}C-choline PET detection rate and serum PSA levels [39]. Several clinicopathological factors of prostate cancer can be statistically significant for ^{11}C-choline uptake, even when the PSA value and kinetics are low [40]. Despite some evidence, ^{18}F-FDG is rarely used in the evaluation of prostate cancer, because ^{18}F-FDG PET has a low sensitivity for the detection of prostate cancer, as exemplified by the fact that its sensitivity for detection of bone metastases is lower than that of bone scintigraphy [41]. This also increases the application value of ^{18}F/^{13}C-choline.

6. Acetate

As with lactate, pyruvate can be converted into acetate through keto acid dehydrogenase. Acetate can serve as an intermediate product of shuttle metabolism in cancer cells that interacts with surrounding cells or is capable of resisting external stress [42]. Studies have shown that cancer cells are capable of adapting to low oxygen environments through the conversion of acetate. Specifically, mitochondria-localized acetyl-CoA synthetases (ACSS 1/2) convert acetate into acetyl-CoA for use in the TCA cycle or fatty acid synthesis [43]. The abnormal expression of ACSS2 has also been observed in several cancers, making it a potential target for cancer therapy [44][45][46]. Acetate, in addition to serving as a buffer for metabolic intermediates, can also play the function of compensating for acidic PH environments through its role in histone acetylation [43].

Similar to choline, acetate is a precursor for lipid biosynthesis [47]. Studies have shown that it is an important bioenergetic fuel for tumor cells. It has been claimed to promote histone acetylation and other epigenetic modifications. Despite the lower circulating concentrations of acetate, it can still surround the intracellular circulation and tumor microenvironment [43]. The difference in kinetics between normal myocardium, normal renal parenchyma, and renal cancer tissue has been proven. Myocardial and normal renal tissue showed rapid washing, consistent with the predominant oxidation to CO_2 through the tricarboxylic acid cycle. In contrast, the tracer was retained in tumor tissue, probably because of the use of ^{11}C-acetate as an important substrate for the generation of membrane lipids [48]. Through comparison of multiple organs and conditions using imaging tools, acetate has been verified as suitable for the detection of prostate cancer.

For prostate cancer, ^{11}C-acetate can be used as a predictive, prognostic, and intermediated endpoint biomarker. ^{11}C-acetate can be detected under low PSA conditions, but it is hard to differentiate between benign prostatic hyperplasia and prostate cancer. In contrast, ^{11}C-acetate PET can be used to assess the regional lymph node and recurrence status [49]. As mentioned previously, the sensitivity of the diagnostic range of ^{11}C-acetate and choline PET probes is important in the evaluation of prostate cancer. Although ^{11}C-acetate has the advantage of low urinary excretion, ^{18}F-choline is more widely used because of its longer physical half-life. ^{11}C-acetate and ^{11}C-

choline can only identify about 50% of recurrence sites, although they both have limitations in patients with PSA levels below 1ng/mL [50].

7. Pivalic Acid

In some clinical studies, glucose is not a suitable tracer, because cells can also produce energy through other metabolic pathways, such as fatty acid oxidation. Some de novo biosynthesis or short-chain fatty acid salvage pathways are important sources of nutrients for cell growth and proliferation [51]. These include acetate and ^{18}F-fluoropivalate (3-^{18}F-fluoro-2,2-dimethylpropionic acid, ^{18}F-FPIA). Unlike acetate, pivalate cannot be oxidized to carbon dioxide in mammalian cells because it carries a *tert*-butyl substituent [52]. Pivalate is esterified in vivo in normal tissue, and the resulting ester enters plasma and is absorbed by cells inhibited by L-carnitine or rapidly eliminated in urine [53]. Dubash et al. evaluated the safety, biodistribution, and internal radiation dosimetry profile of ^{18}F-FPIA in healthy volunteers [54]. A current phase 2 clinical trial (NCT04717674) has enrolled some solid tumor patients who are undergoing ^{18}F-FIPA PET imaging. Their ^{18}F-FIPA tumor uptake will be calculated, and several histological markers of tumor metabolism measured. These biomarkers include Ki-67 and typical enzymes related to fatty acids (SDHA, CPT1/CAT1, CACT, SLC22A2, SLC22A5, and SLC25A20).

8. Cyclobutanecarboxylic Acid

Fluoro-18 (^{18}F) fluciclovine (anti-1-amino-3–^{18}F-fluorocyclobutane-1-carboxylic acid [FACBC]) is a radiolabeled amino acid analog that is upregulated by amino acid transport in a variety of cancer cells, and prostate cancer in particular [55][56][57]. With its low radioactivity background, it is effective for detecting prostate progression, even in cases of lymph node or bone metastasis below 5 mm [58].

It can be taken up through the human L-type amino acid transporter and alanine-serin-cysteine transporter systems [59]. By the same principle, FACBC is analogous to FDG in that it is a metabolite that, when taken up by cells, cannot be metabolized and remains in the tumor area. The sample application principle also includes ^{18}FDG, FACBC, and ^{11}C-choline. They each use glucose transporter (GLUTs), L-type amino acid transporter (LAT/ASCT2), and choline transporter, respectively. The ^{68}Ga PSMA-11 and ^{111}In-Capromab pendetides target the specific antigen PSMA [60].

9. Methionine

Methionine is a natural essential amino acid involved in various types of biosynthesis. It is possible for methionine cycle biosynthesis to convert methionine into S-adenosylmethionine (SAM) in order for methyl donors to be synthesized for genetic processes through methionine adenosyltransferase (MAT) [61][62]. The Hoffman effect is a phenomenon that describes proliferating cells relying on methionine for growth [63]. Methionine has been found to be present in high amounts in certain cancer cells [64]. Compared with normal cells, cancer cells deprived of exogenous methionine in the environment grow and move more slowly [65]. Consequently, labeling methionine is

considered an effective method for identifying cancer cells. For use as a radiotracer, methionine is labeled using carbon-11 and its distribution is usually detected using PET. MET images of brain tumors often show increased uptake in tumors with the presence of amino acid transporters (sodium-independent L-transporters, LAT1, 2, and 3), MET metabolism, tumor vascular bed-dependent blood flow, microvessel density, and blood–brain barrier distribution. This property has made ^{11}C-Met a popular imaging agent in brain cancer patients [66]. The conditions to which it has been applied range from genetic alterations and relapse status to post-chemotherapy evaluations [67][68][69][70][71][72].

Park et al. also described the application of ^{11}C-Met in intracranial germinoma, observing that ^{11}C-Met PET parameters had a significant association with tumor location, sex, *KRAS* variant, and symptoms [73]. Morales-Lozano et al. also compared ^{11}C-Met and ^{18}F-FDG in multiple myeloma, and they confirmed that ^{11}C-Met PET/CT was more sensitive than ^{18}F-FDG for evaluation of myeloma tumors [74]. Currently, a clinical trial is underway to evaluate the response of a more comprehensive range of cancer types (NCT00840047).

10. Glutamine

Glutamine is the most abundant and versatile amino acid in the body. Many metabolic events are expected to be associated with glutamine use. Even in immune cells, its frequency of use approaches or exceeds that of glucose. In energy metabolism, glutamine is a supplementary pathway other than glucose and can be involved in the TCA cycle and events within the mitochondria. Glutamine is an essential nutrient for lymphocyte proliferation and cytokine production, macrophage phagocytosis and secretory activities, as well as neutrophil bacterial killing [75].

As well as its role as an energy source, glutamine also plays an important role in maintaining a balance between the pressures produced by antioxidants and oxidative stress. Meanwhile, it has been found that Glutamine is reliant on Methionine in some cancer cells [76]. This phenomenon is especially evident in clear cell renal cell carcinomas and breast cancer, in which both tumor microenvironment cells and tumor cells will deplete glutamine levels. This depletion limits the harmful effects of peripheral immune cells on cancer [77][78]. As a result, targeting Glutamine selectively is an effective method of diagnosis.

To evaluate the safety and tumor imaging characteristics of fluorine 18-(*2S,4R*)-4-gluoroglutamine (FGln), the Dunphy Group performed scans on cancer patients [79]. Cohen et al. reported that ^{11}C-Gln could be applied to metastatic colorectal cancer. The status quo is that some targeted therapies are used in combination with glutamine metabolism inhibitors, but the study lacked appropriate diagnostic tools for assessment of early response. Therefore, calculated glutamine influx and glutamate efflux (^{11}C-Gln and ^{18}F-FSPG, respectively) have been recruited for further safety and biodistribution evaluation (NCT03263429) [80]. Glioma study indicates that although ^{18}F-FGln is not superior to many current neuroimaging modalities, it may provide complementary biological information specifically about metabolic nutrient uptake relevant to glioma pathology [81]. ^{18}F-FGln uptake in gliomas is positively correlated with glioma progression, and can be indicative of gene alterations (*PTEN* or *IDH1*) events or response to chemotherapy or radiation therapy. More recently, the glutamine-derived development, ^{18}F-labeled glutamate (4*S*)-4-(3-^{18}F-fluoropropyl)-1-glutamate, has been considered a PET tracer in

preclinical models and human subjects [82]. However, the disadvantages of ^{18}F-FGln still include neuroinflammation or disruption of the BBB that cannot be clearly observed [81].

11. Fluoropropyl-L-Glutamic Acid (FSPG)

Glutamic acid and glutamine are both interconvertible. Furthermore, *N*-acetylglutamate, α-ketoglutarate, 1-Pyrroline-5-carvoxylate, *N*-Formimino-L-glutamate, and *N*-acetylaspartylglutamic acid (NAAG) can produce glutamic acid through their corresponding enzymes [83]. Glutamic acid and glutamine form the glutamate metabolism that comprises several reversible and irreversible reactions.

FSPG could be applied to measure system XC-transporter activity, because it contributes to the important function of glutathione biosynthesis and the glutaminolytic pathway. These transporter families include SLC1A5, SLC38A1/A2, and SLC7A11 [84]. Unlike glycolysis, the glutaminolytic, glutathione biosynthesis, and redox balance pathways are dominant metabolic reprogramming events in cancer [85]. According to previous research, it can be detected and quantified in several types of cancer, including head and neck, colorectal, and non-Hodgkin lymphoma, and can play a complementary role in insignificant and ineffective types of ^{18}FDG. There are many unknowns in the related research, but it has development potential for future systems.

12. L-Tyrosine

L-tyrosine arises from amino acid biosynthesis and is considered one of the necessary amino acids. In addition to being associated with Huntington's disease and phenylketonuria, abnormal tyrosine metabolism has also been demonstrated to be associated with malignancy in several cancers [86]. It is evident from the method of blood detection that tyrosine levels will increase abnormally in HCC [87]. Based on the analysis of large sets of data such as TCGA and GEO, it appears there is a strong correlation between genes associated with tyrosine metabolism and poor prognosis in HCC [88]. A study conducted by Sun also suggests that acetyl-CoA generated by tyrosine metabolism may promote stemness activity in HCCs, thereby making them resistant to therapeutic treatment [89].

With amino acid PET, one can obtain information on the metabolism of tumor cells, which is complementary to structural imaging using magnetic resonance images [90]. Common amino acid-type radiotracers include ^{18}F-FET and ^{11}C-Met. Because ^{18}F-FET has lower uptake by inflammatory cells than ^{11}C-methionine or 18F-FDG, it is useful for differentiating tumors from treatment-induced necrosis [91]. Labeled with L-tyrosine fluoroine-18 fluorine, the approach with MRI can achieve 93% sensitivity and 94% specificity in glioma tissue [92].

In current glioblastoma treatments, temozolomide (TMZ) is considered the standard chemotherapy regimen for patients, but it leads to drug resistance and survival prolongation is limited. However, ^{18}F-FET may be a valuable tool for predicting the outcome of therapy before the commencement of TMZ maintenance therapy [93]. Merging this evidence, ^{18}F-FET has been identified as having a good diagnostic performance for the initial assessment of patients with new isolated brain lesions [94]. A previous retrospective study also claimed that a combination of static

and kinetic ^{18}F-FET parameters achieved a higher diagnostic accuracy than conventional MRI in distinguishing between recurrent or progressive disease and treatment-related changes [95].

13. Thymidine

Thymidine is the DNA nucleoside that pairs with deoxyadenosine in double-stranded DNA [96]. In cell biology, it is used to synchronize cells in the S phase, so its production is closely related to the cell cycle [97]. Cancer cells often exhibit abnormal cell proliferation, and many treatments have been developed to inhibit genetic replication. Inhibitors of thymidylate synthase (TS), such as 5-fluorouracil (5-FU), are available [98]. It has been demonstrated that combining 5-FU and leucovorin or oxaliplatin significantly increases the chance of TS and improves outcomes, but it also has great side effects on patients with advanced CRC [99][100]. It is, therefore, beneficial to develop early detection of patients in order to increase the diagnosis rate and formulate further treatment strategies.

In addition to several common thymidine analogs (BrdU and EdU) that have proliferation monitors, the thymidine analog 3′-deoxy-3′[^{18}F] fluorothymidine (FLT) has been developed as a proliferation marker for cancer research. Interestingly, the rate-limiting enzyme of FLT metabolism, the pyrimidine-metabolizing enzyme thymidine kinase-1 (TK-1), is overexpressed in pancreatic cancer cell lines and pancreatic cancer [101]. ^{18}F-FLT is transported through the cell membrane and trapped inside the cell after phosphorylation by thymidine kinase 1 (TK1). Although ^{18}F-FLT is not incorporated into DNA, it is still considered a surrogate marker of cellular proliferation because TK1 activity is closely regulated by the cell cycle [102]. A close relationship could be demonstrated between tumor retention and cell proliferation, suggesting that ^{18}F-FLT is a promising marker for monitoring treatment response. Unlike ^{18}F-FDG, ^{18}F-FLT is not taken up by inflammatory cells, which could reduce the rate of false positive findings in both in pancreatitis and inflammatory tissue after therapy [101]. A comparative study revealed that ^{18}F-FLT was more sensitive than ^{18}F-FDG and ^{18}F-fluorethylcholine in a human pancreatic xenograft model using SCID mice [101]. Similarly, TK-1 and DTYMK kinase and some related transporters, SLC28A1 and SLC29A3, increased significantly in the PDAC group [101]. The use of ^{18}F-FLT is not limited to pancreatic cancer, but has some additional applications in different types and combinations. The Cieslak group has shown that pharmacological ascorbate ($AscH^-$) induces cytotoxicity and oxidative stress in pancreatic cancer and then contributes to the radiosensitizer function monitored by ^{18}F-FLT PET [103]. Collet et al. also claimed that ^{18}F-fluoro-$_L$-thymidine could provide an additional indicator for the staging of gliomas, in particular distinguishing between stage II or stage III (low-grade glioma) and stage IV (glioblastomas) [104]. Furthermore, there is an ongoing study to evaluate 18F-FLT uptake in non-small cell lung cancer following pemetrex treatment. Because of the response and activation of the dexamethasone/pemetrexed thymidine salvage pathway inhibited by dexamethasone/pemetrexed [105], the authors hypothesize that this strategy can be detected as an increase in FLT tumor uptake that subsequently decreases with reduced proliferation. In this study, the FLT response had a good overall survival rate that was twice that of no response. However, the study needs to recruit more case numbers and statistics with clinicopathological factors [106].

14. Dihydroxyphenylalanine (DOPA)

In addition to the well-known carboxylate metabolism, there is fatty acid biosynthesis and amino acid biosynthesis. Neurotransmitters are considered an important aspect, involving signaling pathways in the brain, reflex actions, nerve networks, memory, emotions, etc. Normal and tumoral neuroendocrine cells can uptake and decarboxylate amine precursors (such as L-DOPA and 5-hydroxytryptophan) to produce biogenic amines, such as catecholamines and serotonin [107]. For neuroendocrine tumors (NET), fluorine-18-dihydroxyphenylalanin (^{18}F-DOPA) has been engineered to capture signals because these tumors can accumulate and decarboxylate biogenic amines. Through activation of large amino acid transporters (LAT, SLC7A5/A8), ^{18}F-DOPA is absorbed into tumors and further decarboxylated by DOPA decarboxylase to produce ^{18}F-DOPAmine, which is then transported by vesicular monoamine transporters (VMAT, SLC18A1/A2) and trapped in cells [108]. ^{18}F-DOPA has comprehensive applications in different neuroendocrine tumors, including medullary thyroid cancer (MTC), pancreatic NET, and paragangliomas/phaeochromocytomas [109]. Furthermore, ^{18}F-DOPA can differentiate between Parkinson's disease and dopaminergic transmission disorder [110]. ^{18}F-DOPA enables presynaptic dopaminergic function to be quantified, and specific regions of linear reduction in ^{18}F-DOPA uptake in idiopathic Parkinson's disease to be observed [110].

In addition to ^{18}F-DOPA, gallium-68-somatostatin analogs (DOTA-NOC, DOTA-TOC or DOTA-TATE) have also shown high diagnostic NET imaging on PET/CT scans targeting the accuracy of the somatostatin receptor (SSR). Several studies have compared the uptake and additional functional activity of SSR PET/CT and ^{18}F-DOPA PET/CT. Although patients with gastroenteropancreatic and thoracic NETs may prefer SSR PET/CT as a priority strategy, ^{18}F-DOPA PET/CT remains another viable option [111].

15. Glucosamine

Glycosylation is a hallmark of various neurological disorders. A current study found that N-linked protein glycosylation in the brain led to glucosamine metabolism through glycogen catabolism [112]. Brain glycogen contains 25% glucosamine, and the mass spectrometry imaging method can reveal the distribution of brain glycogen [112]. Additionally, glycogen is a branched glucose polymer that is synthesized from the activated glucose donor, uridine diphosphoglucose (UDP) [112]. In some cancer cells, researchers can observe that the cell is deficient in energy stores that require glucose uptake. There is also evidence that glycogen is more than a glucose cache, and is a critical storage macromolecule for the brain protein N-glycosylation, which impacts myriad subsequent cellular processes. Therefore, a fluorescent tool labeled fluorine-18 has been developed to detect glycogen [113].

Returning to the metabolic background, the glucosamine analog, N- (methyl-2-fluoroethyl) -1H- [12,3] triazole-4-yl) glucosamine (NFTG) has been applied to some animal models. Witney's group confirmed that some cancer cells do not have high glucose uptake, but have strong glucose storage and glycogen (glycogenesis). Annotation of glycogenogenesis, glycogen, and glycogen synthase 1 expression in cancer cells with ^{18}F-NFTG is advantageous in understanding the potential ability of ^{18}F-NFTG to specifically image certain quiescent cells (G_0–G_1 phase).

Furthermore, ^{18}F-NFTG provides higher-specificity tumor imaging under inflammatory conditions than ^{18}F-FDG [114].

References

1. Aroldi, F.; Lord, S.R. Window of opportunity clinical trial designs to study cancer metabolism. Br. J. Cancer 2020, 122, 45–51.
2. Ancey, P.B.; Contat, C.; Meylan, E. Glucose transporters in cancer—From tumor cells to the tumor microenvironment. FEBS J. 2018, 285, 2926–2943.
3. Kim, Y.H.; Jeong, D.C.; Pak, K.; Han, M.E.; Kim, J.Y.; Liangwen, L.; Kim, H.J.; Kim, T.W.; Kim, T.H.; Hyun, D.W.; et al. SLC2A2 (GLUT2) as a novel prognostic factor for hepatocellular carcinoma. Oncotarget 2017, 8, 68381–68392.
4. Chai, Y.J.; Yi, J.W.; Oh, S.W.; Kim, Y.A.; Yi, K.H.; Kim, J.H.; Lee, K.E. Upregulation of SLC2 (GLUT) family genes is related to poor survival outcomes in papillary thyroid carcinoma: Analysis of data from The Cancer Genome Atlas. Surgery 2017, 161, 188–194.
5. Flavahan, W.A.; Wu, Q.; Hitomi, M.; Rahim, N.; Kim, Y.; Sloan, A.E.; Weil, R.J.; Nakano, I.; Sarkaria, J.N.; Stringer, B.W.; et al. Brain tumor initiating cells adapt to restricted nutrition through preferential glucose uptake. Nat. Neurosci. 2013, 16, 1373–1382.
6. Han, A.L.; Veeneman, B.A.; El-Sawy, L.; Day, K.C.; Day, M.L.; Tomlins, S.A.; Keller, E.T. Fibulin-3 promotes muscle-invasive bladder cancer. Oncogene 2017, 36, 5243–5251.
7. Lord, S.R.; Cheng, W.C.; Liu, D.; Gaude, E.; Haider, S.; Metcalf, T.; Patel, N.; Teoh, E.J.; Gleeson, F.; Bradley, K.; et al. Integrated Pharmacodynamic Analysis Identifies Two Metabolic Adaption Pathways to Metformin in Breast Cancer. Cell Metab. 2018, 28, 679–688.e674.
8. Lunt, S.Y.; Vander Heiden, M.G. Aerobic glycolysis: Meeting the metabolic requirements of cell proliferation. Annu. Rev. Cell Dev. Biol. 2011, 27, 441–464.
9. Cox, B.L.; Mackie, T.R.; Eliceiri, K.W. The sweet spot: FDG and other 2-carbon glucose analogs for multi-modal metabolic imaging of tumor metabolism. Am. J. Nucl. Med. Mol. Imaging 2015, 5, 1–13.
10. Gallamini, A.; Zwarthoed, C.; Borra, A. Positron Emission Tomography (PET) in Oncology. Cancers 2014, 6, 1821–1889.
11. Mirus, M.; Tokalov, S.V.; Abramyuk, A.; Heinold, J.; Prochnow, V.; Zöphel, K.; Kotzerke, J.; Abolmaali, N. Noninvasive assessment and quantification of tumor vascularization using FDG-PET/CT and CE-CT in a tumor model with modifiable angiogenesis-an animal experimental prospective cohort study. EJNMMI Res. 2019, 9, 55.

12. Namavari, M.; Cheng, Z.; Zhang, R.; De, A.; Levi, J.; Hoerner, J.K.; Yaghoubi, S.S.; Syud, F.A.; Gambhir, S.S. A novel method for direct site-specific radiolabeling of peptides using FDG. Bioconjug. Chem. 2009, 20, 432–436.
13. Şenışık, A.M.; İçhedef, Ç.; Kılçar, A.Y.; Uçar, E.; Arı, K.; Göksoy, D.; Parlak, Y.; Sayıt Bilgin, B.E.; Teksöz, S. One-step conjugation of glycylglycine with FDG and a pilot PET imaging study. J. Radioanal. Nucl. Chem. 2018, 316, 457–463.
14. Sprinz, C.; Altmayer, S.; Zanon, M.; Watte, G.; Irion, K.; Marchiori, E.; Hochhegger, B. Effects of blood glucose level on 18F-FDG uptake for PET/CT in normal organs: A systematic review. PLoS ONE 2018, 13, e0193140.
15. Boellaard, R.; Delgado-Bolton, R.; Oyen, W.J.; Giammarile, F.; Tatsch, K.; Eschner, W.; Verzijlbergen, F.J.; Barrington, S.F.; Pike, L.C.; Weber, W.A.; et al. FDG PET/CT: EANM procedure guidelines for tumour imaging: Version 2.0. Eur. J. Nucl. Med. Mol. Imaging 2015, 42, 328–354.
16. Lee, T.C.; Alessio, A.M.; Miyaoka, R.M.; Kinahan, P.E. Morphology supporting function: Attenuation correction for SPECT/CT, PET/CT, and PET/MR imaging. Q. J. Nucl. Med. Mol. Imaging 2016, 60, 25–39.
17. de la Cruz-López, K.G.; Castro-Muñoz, L.J.; Reyes-Hernández, D.O.; García-Carrancá, A.; Manzo-Merino, J. Lactate in the Regulation of Tumor Microenvironment and Therapeutic Approaches. Front. Oncol. 2019, 9, 1143.
18. Kim, S.H.; Baek, K.H. Regulation of Cancer Metabolism by Deubiquitinating Enzymes: The Warburg Effect. Int. J. Mol. Sci. 2021, 22, 6173.
19. Witney, T.H.; Kettunen, M.I.; Day, S.E.; Hu, D.E.; Neves, A.A.; Gallagher, F.A.; Fulton, S.M.; Brindle, K.M. A comparison between radiolabeled fluorodeoxyglucose uptake and hyperpolarized (13)C-labeled pyruvate utilization as methods for detecting tumor response to treatment. Neoplasia 2009, 11, 574–582, 571 p following 582.
20. Serrao, E.M.; Kettunen, M.I.; Rodrigues, T.B.; Lewis, D.Y.; Gallagher, F.A.; Hu, D.E.; Brindle, K.M. Analysis of (13) C and (14) C labeling in pyruvate and lactate in tumor and blood of lymphoma-bearing mice injected with (13) C- and (14) C-labeled pyruvate. NMR Biomed. 2018, 31, e3901.
21. Park, J.W.; Kim, J.H.; Kim, S.K.; Kang, K.W.; Park, K.W.; Choi, J.I.; Lee, W.J.; Kim, C.M.; Nam, B.H. A prospective evaluation of 18F-FDG and 11C-acetate PET/CT for detection of primary and metastatic hepatocellular carcinoma. J. Nucl. Med. 2008, 49, 1912–1921.
22. Barretina, J.; Caponigro, G.; Stransky, N.; Venkatesan, K.; Margolin, A.A.; Kim, S.; Wilson, C.J.; Lehár, J.; Kryukov, G.V.; Sonkin, D.; et al. The Cancer Cell Line Encyclopedia enables predictive modelling of anticancer drug sensitivity. Nature 2012, 483, 603–607.

23. Sørensen, M.; Frisch, K.; Bender, D.; Keiding, S. The potential use of 2-fluoro-2-deoxy-D-galactose as a PET/CT tracer for detection of hepatocellular carcinoma. Eur. J. Nucl. Med. Mol. Imaging 2011, 38, 1723–1731.
24. Sørensen, M. Determination of hepatic galactose elimination capacity using 2-fluoro-2-deoxy-D-galactose PET/CT: Reproducibility of the method and metabolic heterogeneity in a normal pig liver model. Scand. J. Gastroenterol. 2011, 46, 98–103.
25. Sørensen, M.; Munk, O.L.; Mortensen, F.V.; Olsen, A.K.; Bender, D.; Bass, L.; Keiding, S. Hepatic uptake and metabolism of galactose can be quantified in vivo by 2-fluoro-2-deoxygalactose positron emission tomography. Am. J. Physiol. Gastrointest. Liver Physiol. 2008, 295, G27–G36.
26. Frisch, K.; Bender, D.; Hansen, S.B.; Keiding, S.; Sørensen, M. Nucleophilic radiosynthesis of 2-fluoro-2-deoxy-D-galactose from Talose triflate and biodistribution in a porcine model. Nucl. Med. Biol. 2011, 38, 477–483.
27. Horsager, J.; Bak-Fredslund, K.; Larsen, L.P.; Villadsen, G.E.; Bogsrud, T.V.; Sørensen, M. Optimal 2-fluoro-2-deoxy-D-galactose PET/CT protocol for detection of hepatocellular carcinoma. EJNMMI Res. 2016, 6, 56.
28. Bak-Fredslund, K.P.; Munk, O.L.; Keiding, S.; Sørensen, M. 2-fluoro-2-deoxy-D-galactose PET/CT of hepatocellular carcinoma is not improved by co-administration of galactose. Nucl. Med. Biol. 2016, 43, 577–580.
29. Spadaro, F.; Ramoni, C.; Mezzanzanica, D.; Miotti, S.; Alberti, P.; Cecchetti, S.; Iorio, E.; Dolo, V.; Canevari, S.; Podo, F. Phosphatidylcholine-specific phospholipase C activation in epithelial ovarian cancer cells. Cancer Res. 2008, 68, 6541–6549.
30. Iorio, E.; Ricci, A.; Bagnoli, M.; Pisanu, M.E.; Castellano, G.; Di Vito, M.; Venturini, E.; Glunde, K.; Bhujwalla, Z.M.; Mezzanzanica, D.; et al. Activation of phosphatidylcholine cycle enzymes in human epithelial ovarian cancer cells. Cancer Res. 2010, 70, 2126–2135.
31. Kwee, S.A.; Sato, M.M.; Kuang, Y.; Franke, A.; Custer, L.; Miyazaki, K.; Wong, L.L. Fluorocholine PET/CT Imaging of Liver Cancer: Radiopathologic Correlation with Tissue Phospholipid Profiling. Mol. Imaging Biol. 2017, 19, 446–455.
32. Kwee, S.A.; Wong, L.; Chan, O.T.M.; Kalathil, S.; Tsai, N. PET/CT with (18)F Fluorocholine as an Imaging Biomarker for Chronic Liver Disease: A Preliminary Radiopathologic Correspondence Study in Patients with Liver Cancer. Radiology 2018, 287, 294–302.
33. Wenz, J.; Arndt, F.; Samnick, S. A new concept for the production of (11)C-labelled radiotracers. EJNMMI Radiopharm. Chem. 2022, 7, 6.
34. Caribé, P.; Vandenberghe, S.; Diogo, A.; Pérez-Benito, D.; Efthimiou, N.; Thyssen, C.; D'Asseler, Y.; Koole, M. Monte Carlo Simulations of the GE Signa PET/MR for Different Radioisotopes. Front. Physiol. 2020, 11, 525575.

35. Boutzios, G.; Sarlanis, H.; Kolindou, A.; Velidaki, A.; Karatzas, T. Primary hyperparathyroidism caused by enormous unilateral water-clear cell parathyroid hyperplasia. BMC Endocr. Disord. 2017, 17, 57.
36. Liu, Y.; Dang, Y.; Huo, L.; Hu, Y.; Wang, O.; Liu, H.; Chang, X.; Liu, Y.; Xing, X.; Li, F.; et al. Preoperative Localization of Adenomas in Primary Hyperparathyroidism: The Value of (11)C-Choline PET/CT in Patients with Negative or Discordant Findings on Ultrasonography and (99m)Tc-Sestamibi SPECT/CT. J. Nucl. Med. 2020, 61, 584–589.
37. Noltes, M.E.; Kruijff, S.; Jansen, L.; Westerlaan, H.E.; Zandee, W.T.; Dierckx, R.; Brouwers, A.H. A retrospective analysis of the diagnostic performance of (11)C-choline PET/CT for detection of hyperfunctioning parathyroid glands after prior negative or discordant imaging in primary hyperparathyroidism. EJNMMI Res. 2021, 11, 32.
38. Welle, C.L.; Cullen, E.L.; Peller, P.J.; Lowe, V.J.; Murphy, R.C.; Johnson, G.B.; Binkovitz, L.A. 11C-Choline PET/CT in Recurrent Prostate Cancer and Nonprostatic Neoplastic Processes. Radiographics 2016, 36, 279–292.
39. Krause, B.J.; Souvatzoglou, M.; Tuncel, M.; Herrmann, K.; Buck, A.K.; Praus, C.; Schuster, T.; Geinitz, H.; Treiber, U.; Schwaiger, M. The detection rate of choline-PET/CT depends on the serum PSA-value in patients with biochemical recurrence of prostate cancer. Eur. J. Nucl. Med. Mol. Imaging 2008, 35, 18–23.
40. Picchio, M.; Castellucci, P. Clinical Indications of C-Choline PET/CT in Prostate Cancer Patients with Biochemical Relapse. Theranostics 2012, 2, 313–317.
41. Bouchelouche, K.; Tagawa, S.T.; Goldsmith, S.J.; Turkbey, B.; Capala, J.; Choyke, P. PET/CT Imaging and Radioimmunotherapy of Prostate Cancer. Semin. Nucl. Med. 2011, 41, 29–44.
42. Bose, S.; Ramesh, V.; Locasale, J.W. Acetate Metabolism in Physiology, Cancer, and Beyond. Trends Cell Biol. 2019, 29, 695–703.
43. Schug, Z.T.; Vande Voorde, J.; Gottlieb, E. The metabolic fate of acetate in cancer. Nat. Rev. Cancer 2016, 16, 708–717.
44. Ling, R.; Chen, G.; Tang, X.; Liu, N.; Zhou, Y.; Chen, D. Acetyl-CoA synthetase 2(ACSS2): A review with a focus on metabolism and tumor development. Discov. Oncol. 2022, 13, 58.
45. Liu, M.; Liu, N.; Wang, J.; Fu, S.; Wang, X.; Chen, D. Acetyl-CoA Synthetase 2 as a Therapeutic Target in Tumor Metabolism. Cancers 2022, 14, 2896.
46. Zhou, Z.; Ren, Y.; Yang, J.; Liu, M.; Shi, X.; Luo, W.; Fung, K.M.; Xu, C.; Bronze, M.S.; Zhang, Y.; et al. Acetyl-Coenzyme A Synthetase 2 Potentiates Macropinocytosis and Muscle Wasting Through Metabolic Reprogramming in Pancreatic Cancer. Gastroenterology 2022, 163, 1281–1293.e1281.

47. Schug, Z.T.; Peck, B.; Jones, D.T.; Zhang, Q.; Grosskurth, S.; Alam, I.S.; Goodwin, L.M.; Smethurst, E.; Mason, S.; Blyth, K.; et al. Acetyl-CoA synthetase 2 promotes acetate utilization and maintains cancer cell growth under metabolic stress. Cancer Cell 2015, 27, 57–71.
48. Shreve, P.; Chiao, P.C.; Humes, H.D.; Schwaiger, M.; Gross, M.D. Carbon-11-acetate PET imaging in renal disease. J. Nucl. Med. 1995, 36, 1595–1601.
49. Spick, C.; Herrmann, K.; Czernin, J. Evaluation of Prostate Cancer with 11C-Acetate PET/CT. J. Nucl. Med. 2016, 57, 30s–37s.
50. Vees, H.; Buchegger, F.; Albrecht, S.; Khan, H.; Husarik, D.; Zaidi, H.; Soloviev, D.; Hany, T.F.; Miralbell, R. 18F-choline and/or 11C-acetate positron emission tomography: Detection of residual or progressive subclinical disease at very low prostate-specific antigen values (<1 ng/mL) after radical prostatectomy. BJU Int. 2007, 99, 1415–1420.
51. Luengo, A.; Gui, D.Y.; Vander Heiden, M.G. Targeting Metabolism for Cancer Therapy. Cell Chem. Biol. 2017, 24, 1161–1180.
52. Brass, E.P. Pivalate-generating prodrugs and carnitine homeostasis in man. Pharmacol. Rev. 2002, 54, 589–598.
53. Kuka, J.; Makrecka, M.; Grinberga, S.; Pugovics, O.; Liepinsh, E.; Dambrova, M. A short-term high-dose administration of sodium pivalate impairs pyruvate metabolism without affecting cardiac function. Cardiovasc. Toxicol. 2012, 12, 298–303.
54. Dubash, S.R.; Keat, N.; Kozlowski, K.; Barnes, C.; Allott, L.; Brickute, D.; Hill, S.; Huiban, M.; Barwick, T.D.; Kenny, L.; et al. Clinical translation of (18)F-fluoropivalate—A PET tracer for imaging short-chain fatty acid metabolism: Safety, biodistribution, and dosimetry in fed and fasted healthy volunteers. Eur. J. Nucl. Med. Mol. Imaging 2020, 47, 2549–2561.
55. Bin, X.; Yong, S.; Kong, Q.F.; Zhao, S.; Zhang, G.Y.; Wu, J.P.; Chen, S.Q.; Zhu, W.D.; Pan, K.H.; Du, M.L.; et al. Diagnostic Performance of PET/CT Using 18F-FACBC in Prostate Cancer: A Meta-Analysis. Front. Oncol. 2019, 9, 1438.
56. Farkas, A.B.; Green, E.D.; Thaggard, A.L.; Vijayakumar, V.; Henegan, J.C.; Lirette, S.T.; Nittala, M.R.; Vijayakumar, S. Initial Institutional Experience with 18F-Fluciclovine PET-CT in Biochemical Recurrence of Prostate Cancer. South Med. J. 2021, 114, 703–707.
57. Wang, K.; Su, R.; Sun, X.; Jiang, J.; Ma, Q. Progress in applications of (18)F-fluciclovine in diagnosis of prostate cancer. Zhong Nan Da Xue Xue Bao Yi Xue Ban 2020, 45, 187–192.
58. Schuster, D.M.; Savir-Baruch, B.; Nieh, P.T.; Master, V.A.; Halkar, R.K.; Rossi, P.J.; Lewis, M.M.; Nye, J.A.; Yu, W.; Bowman, F.D.; et al. Detection of recurrent prostate carcinoma with anti-1-amino-3-18F-fluorocyclobutane-1-carboxylic acid PET/CT and 111In-capromab pendetide SPECT/CT. Radiology 2011, 259, 852–861.

59. Movahedi, P.; Merisaari, H.; Perez, I.M.; Taimen, P.; Kemppainen, J.; Kuisma, A.; Eskola, O.; Teuho, J.; Saunavaara, J.; Pesola, M.; et al. Prediction of prostate cancer aggressiveness using (18)F-Fluciclovine (FACBC) PET and multisequence multiparametric MRI. Sci. Rep. 2020, 10, 9407.

60. Alberts, I.L.; Seide, S.E.; Mingels, C.; Bohn, K.P.; Shi, K.; Zacho, H.D.; Rominger, A.; Afshar-Oromieh, A. Comparing the diagnostic performance of radiotracers in recurrent prostate cancer: A systematic review and network meta-analysis. Eur. J. Nucl. Med. Mol. Imaging 2021, 48, 2978–2989.

61. Hayashi, T.; Teruya, T.; Chaleckis, R.; Morigasaki, S.; Yanagida, M. S-Adenosylmethionine Synthetase Is Required for Cell Growth, Maintenance of G0 Phase, and Termination of Quiescence in Fission Yeast. iScience 2018, 5, 38–51.

62. Sanderson, S.M.; Gao, X.; Dai, Z.; Locasale, J.W. Methionine metabolism in health and cancer: A nexus of diet and precision medicine. Nat. Rev. Cancer 2019, 19, 625–637.

63. Hoffman, R.M. Development of recombinant methioninase to target the general cancer-specific metabolic defect of methionine dependence: A 40-year odyssey. Expert Opin. Biol. Ther. 2015, 15, 21–31.

64. Cavuoto, P.; Fenech, M.F. A review of methionine dependency and the role of methionine restriction in cancer growth control and life-span extension. Cancer Treat. Rev. 2012, 38, 726–736.

65. Jeon, H.; Kim, J.H.; Lee, E.; Jang, Y.J.; Son, J.E.; Kwon, J.Y.; Lim, T.G.; Kim, S.; Park, J.H.; Kim, J.E.; et al. Methionine deprivation suppresses triple-negative breast cancer metastasis in vitro and in vivo. Oncotarget 2016, 7, 67223–67234.

66. Sun, A.; Liu, X.; Tang, G. Carbon-11 and Fluorine-18 Labeled Amino Acid Tracers for Positron Emission Tomography Imaging of Tumors. Front. Chem. 2017, 5, 124.

67. Glaudemans, A.W.; Enting, R.H.; Heesters, M.A.; Dierckx, R.A.; van Rheenen, R.W.; Walenkamp, A.M.; Slart, R.H. Value of 11C-methionine PET in imaging brain tumours and metastases. Eur. J. Nucl. Med. Mol. Imaging 2013, 40, 615–635.

68. Hotta, M.; Minamimoto, R.; Miwa, K. 11C-methionine-PET for differentiating recurrent brain tumor from radiation necrosis: Radiomics approach with random forest classifier. Sci. Rep. 2019, 9, 15666.

69. Nakajima, R.; Kimura, K.; Abe, K.; Sakai, S. (11)C-methionine PET/CT findings in benign brain disease. Jpn. J. Radiol. 2017, 35, 279–288.

70. Nakajo, K.; Uda, T.; Kawashima, T.; Terakawa, Y.; Ishibashi, K.; Tsuyuguchi, N.; Tanoue, Y.; Nagahama, A.; Uda, H.; Koh, S.; et al. Maximum 11C-methionine PET uptake as a prognostic imaging biomarker for newly diagnosed and untreated astrocytic glioma. Sci. Rep. 2022, 12, 546.

71. Wang, Y.; Rapalino, O.; Heidari, P.; Loeffler, J.; Shih, H.A.; Oh, K.; Mahmood, U. C11 Methionine PET (MET-PET) Imaging of Glioblastoma for Detecting Postoperative Residual Disease and Response to Chemoradiation Therapy. Int. J. Radiat. Oncol. Biol. Phys. 2018, 102, 1024–1028.
72. Zhou, W.; Zhou, Z.; Wen, J.; Xie, F.; Zhu, Y.; Zhang, Z.; Xiao, J.; Chen, Y.; Li, M.; Guan, Y.; et al. A Nomogram Modeling (11)C-MET PET/CT and Clinical Features in Glioma Helps Predict IDH Mutation. Front. Oncol. 2020, 10, 1200.
73. Park, Y.J.; Lee, J.W.; Cho, H.W.; Choe, Y.S.; Lee, K.H.; Choi, J.Y.; Sung, K.W.; Moon, S.H. Value of C-11 methionine PET/CT in patients with intracranial germinoma. PLoS ONE 2022, 17, e0263690.
74. Morales-Lozano, M.I.; Viering, O.; Samnick, S.; Rodriguez-Otero, P.; Buck, A.K.; Marcos-Jubilar, M.; Rasche, L.; Prieto, E.; Kortüm, K.M.; San-Miguel, J.; et al. (18)F-FDG and (11)C-Methionine PET/CT in Newly Diagnosed Multiple Myeloma Patients: Comparison of Volume-Based PET Biomarkers. Cancers 2020, 12, 1042.
75. Cruzat, V.; Macedo Rogero, M.; Noel Keane, K.; Curi, R.; Newsholme, P. Glutamine: Metabolism and Immune Function, Supplementation and Clinical Translation. Nutrients 2018, 10, 1564.
76. Shroff, E.H.; Eberlin, L.S.; Dang, V.M.; Gouw, A.M.; Gabay, M.; Adam, S.J.; Bellovin, D.I.; Tran, P.T.; Philbrick, W.M.; Garcia-Ocana, A.; et al. MYC oncogene overexpression drives renal cell carcinoma in a mouse model through glutamine metabolism. Proc. Natl. Acad. Sci. USA 2015, 112, 6539–6544.
77. Edwards, D.N.; Ngwa, V.M.; Raybuck, A.L.; Wang, S.; Hwang, Y.; Kim, L.C.; Cho, S.H.; Paik, Y.; Wang, Q.; Zhang, S.; et al. Selective glutamine metabolism inhibition in tumor cells improves antitumor T lymphocyte activity in triple-negative breast cancer. J. Clin. Investig. 2021, 131, e140100.
78. Fu, Q.; Xu, L.; Wang, Y.; Jiang, Q.; Liu, Z.; Zhang, J.; Zhou, Q.; Zeng, H.; Tong, S.; Wang, T.; et al. Tumor-associated Macrophage-derived Interleukin-23 Interlinks Kidney Cancer Glutamine Addiction with Immune Evasion. Eur. Urol. 2019, 75, 752–763.
79. Dunphy, M.P.S.; Harding, J.J.; Venneti, S.; Zhang, H.; Burnazi, E.M.; Bromberg, J.; Omuro, A.M.; Hsieh, J.J.; Mellinghoff, I.K.; Staton, K.; et al. In Vivo PET Assay of Tumor Glutamine Flux and Metabolism: In-Human Trial of (18)F-(2S,4R)-4-Fluoroglutamine. Radiology 2018, 287, 667–675.
80. Cohen, A.S.; Grudzinski, J.; Smith, G.T.; Peterson, T.E.; Whisenant, J.G.; Hickman, T.L.; Ciombor, K.K.; Cardin, D.; Eng, C.; Goff, L.W.; et al. First-in-Human PET Imaging and Estimated Radiation Dosimetry of l--Glutamine in Patients with Metastatic Colorectal Cancer. J. Nucl. Med. 2022, 63, 36–43.
81. Venneti, S.; Dunphy, M.P.; Zhang, H.; Pitter, K.L.; Zanzonico, P.; Campos, C.; Carlin, S.D.; La Rocca, G.; Lyashchenko, S.; Ploessl, K.; et al. Glutamine-based PET imaging facilitates

enhanced metabolic evaluation of gliomas in vivo. Sci. Transl. Med. 2015, 7, 274ra217.

82. Baek, S.; Mueller, A.; Lim, Y.S.; Lee, H.C.; Lee, Y.J.; Gong, G.; Kim, J.S.; Ryu, J.S.; Oh, S.J.; Lee, S.J.; et al. (4S)-4-(3-18F-fluoropropyl)-L-glutamate for imaging of xC transporter activity in hepatocellular carcinoma using PET: Preclinical and exploratory clinical studies. J. Nucl. Med. 2013, 54, 117–123.
83. Yelamanchi, S.D.; Jayaram, S.; Thomas, J.K.; Gundimeda, S.; Khan, A.A.; Singhal, A.; Keshava Prasad, T.S.; Pandey, A.; Somani, B.L.; Gowda, H. A pathway map of glutamate metabolism. J. Cell Commun. Signal 2016, 10, 69–75.
84. Zhu, L.; Ploessl, K.; Zhou, R.; Mankoff, D.; Kung, H.F. Metabolic Imaging of Glutamine in Cancer. J. Nucl. Med. 2017, 58, 533–537.
85. Hensley, C.T.; Wasti, A.T.; DeBerardinis, R.J. Glutamine and cancer: Cell biology, physiology, and clinical opportunities. J. Clin. Investig. 2013, 123, 3678–3684.
86. Herman, S.; Niemelä, V.; Emami Khoonsari, P.; Sundblom, J.; Burman, J.; Landtblom, A.M.; Spjuth, O.; Nyholm, D.; Kultima, K. Alterations in the tyrosine and phenylalanine pathways revealed by biochemical profiling in cerebrospinal fluid of Huntington’s disease subjects. Sci. Rep. 2019, 9, 4129.
87. Baumann, U.; Duhme, V.; Auth, M.K.; McKiernan, P.J.; Holme, E. Lectin-reactive alpha-fetoprotein in patients with tyrosinemia type I and hepatocellular carcinoma. J. Pediatr. Gastroenterol. Nutr. 2006, 43, 77–82.
88. Nguyen, T.N.; Nguyen, H.Q.; Le, D.H. Unveiling prognostics biomarkers of tyrosine metabolism reprogramming in liver cancer by cross-platform gene expression analyses. PLoS ONE 2020, 15, e0229276.
89. Sun, L.; Zhang, L.; Chen, J.; Li, C.; Sun, H.; Wang, J.; Xiao, H. Activation of Tyrosine Metabolism in CD13+ Cancer Stem Cells Drives Relapse in Hepatocellular Carcinoma. Cancer Res. Treat. 2020, 52, 604–621.
90. Lohmann, P.; Werner, J.M.; Shah, N.J.; Fink, G.R.; Langen, K.J.; Galldiks, N. Combined Amino Acid Positron Emission Tomography and Advanced Magnetic Resonance Imaging in Glioma Patients. Cancers 2019, 11, 153.
91. Spaeth, N.; Wyss, M.T.; Weber, B.; Scheidegger, S.; Lutz, A.; Verwey, J.; Radovanovic, I.; Pahnke, J.; Wild, D.; Westera, G.; et al. Uptake of 18F-fluorocholine, 18F-fluoroethyl-L-tyrosine, and 18F-FDG in acute cerebral radiation injury in the rat: Implications for separation of radiation necrosis from tumor recurrence. J. Nucl. Med. 2004, 45, 1931–1938.
92. Pauleit, D.; Floeth, F.; Hamacher, K.; Riemenschneider, M.J.; Reifenberger, G.; Müller, H.W.; Zilles, K.; Coenen, H.H.; Langen, K.J. O-(2-fluoroethyl)-L-tyrosine PET combined with MRI improves the diagnostic assessment of cerebral gliomas. Brain 2005, 128, 678–687.

93. Baguet, T.; Verhoeven, J.; De Vos, F.; Goethals, I. Cost-Effectiveness of Fluoroethyl-L-Tyrosine for Temozolomide Therapy Assessment in Patients With Glioblastoma. Front. Oncol. 2019, 9, 814.
94. Dunet, V.; Rossier, C.; Buck, A.; Stupp, R.; Prior, J.O. Performance of 18F-fluoro-ethyl-tyrosine (18F-FET) PET for the differential diagnosis of primary brain tumor: A systematic review and Metaanalysis. J. Nucl. Med. 2012, 53, 207–214.
95. Galldiks, N.; Stoffels, G.; Filss, C.; Rapp, M.; Blau, T.; Tscherpel, C.; Ceccon, G.; Dunkl, V.; Weinzierl, M.; Stoffel, M.; et al. The use of dynamic O-(2-18F-fluoroethyl)-l-tyrosine PET in the diagnosis of patients with progressive and recurrent glioma. Neuro Oncol. 2015, 17, 1293–1300.
96. Cavanagh, B.L.; Walker, T.; Norazit, A.; Meedeniya, A.C. Thymidine analogues for tracking DNA synthesis. Molecules 2011, 16, 7980–7993.
97. Chen, G.; Deng, X. Cell Synchronization by Double Thymidine Block. Bio Protoc. 2018, 8, e2994.
98. Longley, D.B.; Harkin, D.P.; Johnston, P.G. 5-fluorouracil: Mechanisms of action and clinical strategies. Nat. Rev. Cancer 2003, 3, 330–338.
99. André, T.; Boni, C.; Mounedji-Boudiaf, L.; Navarro, M.; Tabernero, J.; Hickish, T.; Topham, C.; Zaninelli, M.; Clingan, P.; Bridgewater, J.; et al. Oxaliplatin, fluorouracil, and leucovorin as adjuvant treatment for colon cancer. N. Engl. J. Med. 2004, 350, 2343–2351.
100. Poon, M.A.; O'Connell, M.J.; Wieand, H.S.; Krook, J.E.; Gerstner, J.B.; Tschetter, L.K.; Levitt, R.; Kardinal, C.G.; Mailliard, J.A. Biochemical modulation of fluorouracil with leucovorin: Confirmatory evidence of improved therapeutic efficacy in advanced colorectal cancer. J. Clin. Oncol. 1991, 9, 1967–1972.
101. von Forstner, C.; Egberts, J.H.; Ammerpohl, O.; Niedzielska, D.; Buchert, R.; Mikecz, P.; Schumacher, U.; Peldschus, K.; Adam, G.; Pilarsky, C.; et al. Gene expression patterns and tumor uptake of 18F-FDG, 18F-FLT, and 18F-FEC in PET/MRI of an orthotopic mouse xenotransplantation model of pancreatic cancer. J. Nucl. Med. 2008, 49, 1362–1370.
102. McKinley, E.T.; Ayers, G.D.; Smith, R.A.; Saleh, S.A.; Zhao, P.; Washington, M.K.; Coffey, R.J.; Manning, H.C. Limits of -FLT PET as a biomarker of proliferation in oncology. PLoS ONE 2013, 8, e58938.
103. Cieslak, J.A.; Sibenaller, Z.A.; Walsh, S.A.; Ponto, L.L.; Du, J.; Sunderland, J.J.; Cullen, J.J. Fluorine-18-Labeled Thymidine Positron Emission Tomography (FLT-PET) as an Index of Cell Proliferation after Pharmacological Ascorbate-Based Therapy. Radiat. Res. 2016, 185, 31–38.
104. Collet, S.; Valable, S.; Constans, J.M.; Lechapt-Zalcman, E.; Roussel, S.; Delcroix, N.; Abbas, A.; Ibazizene, M.; Bernaudin, M.; Barré, L.; et al. -fluoro-L-thymidine PET and advanced MRI for preoperative grading of gliomas. Neuroimage Clin. 2015, 8, 448–454.

105. Chen, X.; Yang, Y.; Katz, S.I. Dexamethasone pretreatment impairs the thymidylate synthase inhibition mediated flare in thymidine salvage pathway activity in non-small cell lung cancer. PLoS ONE 2018, 13, e0202384.

106. Aravind, P.; Popat, S.; Barwick, T.D.; Soneji, N.; Lythgoe, M.; Lozano-kuehne, J.; Sreter, K.B.; Bergqvist, M.; Patel, N.H.; Aboagye, E.O.; et al. Fluorothymidine(FLT)-PET imaging of thymidine kinase 1 pharmacodynamics in non-small cell lung cancer treated with pemetrexed. J. Clin. Oncol. 2022, 40, 3070.

107. Volante, M.; Righi, L.; Berruti, A.; Rindi, G.; Papotti, M. The pathological diagnosis of neuroendocrine tumors: Common questions and tentative answers. Virchows. Arch. 2011, 458, 393–402.

108. Jager, P.L.; Chirakal, R.; Marriott, C.J.; Brouwers, A.H.; Koopmans, K.P.; Gulenchyn, K.Y. 6-L-18F-fluorodihydroxyphenylalanine PET in neuroendocrine tumors: Basic aspects and emerging clinical applications. J. Nucl. Med. 2008, 49, 573–586.

109. Santhanam, P.; Taïeb, D. Role of (18) F-FDOPA PET/CT imaging in endocrinology. Clin. Endocrinol. 2014, 81, 789–798.

110. Stormezand, G.N.; Chaves, L.T.; Vállez García, D.; Doorduin, J.; De Jong, B.M.; Leenders, K.L.; Kremer, B.P.H.; Dierckx, R. Intrastriatal gradient analyses of 18F-FDOPA PET scans for differentiation of Parkinsonian disorders. Neuroimage Clin. 2020, 25, 102161.

111. Treglia, G.; Cocciolillo, F.; de Waure, C.; Di Nardo, F.; Gualano, M.R.; Castaldi, P.; Rufini, V.; Giordano, A. Diagnostic performance of 18F-dihydroxyphenylalanine positron emission tomography in patients with paraganglioma: A meta-analysis. Eur. J. Nucl. Med. Mol. Imaging 2012, 39, 1144–1153.

112. Sun, R.C.; Young, L.E.A.; Bruntz, R.C.; Markussen, K.H.; Zhou, Z.; Conroy, L.R.; Hawkinson, T.R.; Clarke, H.A.; Stanback, A.E.; Macedo, J.K.A.; et al. Brain glycogen serves as a critical glucosamine cache required for protein glycosylation. Cell Metab. 2021, 33, 1404–1417.e1409.

113. Allott, L.; Brickute, D.; Chen, C.; Braga, M.; Barnes, C.; Wang, N.; Aboagye, E.O. Development of a fluorine-18 radiolabelled fluorescent chalcone: Evaluated for detecting glycogen. EJNMMI Radiopharm. Chem. 2020, 5, 17.

114. Witney, T.H.; Carroll, L.; Alam, I.S.; Chandrashekran, A.; Nguyen, Q.D.; Sala, R.; Harris, R.; DeBerardinis, R.J.; Agarwal, R.; Aboagye, E.O. A novel radiotracer to image glycogen metabolism in tumors by positron emission tomography. Cancer Res. 2014, 74, 1319–1328.